11th World Congress on Structural and Multidisciplinary Optimization
7th - 12th, June 2015, Sydney Australia

Shape Optimisation of a Gas Injector

Ruber Arley Ruiz-Mesa[1], Manuel Julio García[2]

[1] EAFIT University, Medellín, Colombia, rruizme@eafit.edu.co
[2] EAFIT University, Medellín, Colombia, mgarcia@eafit.edu.co

1. Abstract
One of the main functions of a gas injector in a domestic oven combustion system is to improve the air-fuel ratio in the burner in order to increase the efficiency in the reaction process (combustion). For such a case, it would be necessary to maximise the primary air that enters into the combustion system and this could be done by redesigning the internal geometry of the injector. By improving this design, it is expected that the chemical reaction process between the fuel and the air becomes cleaner since the mixture inside the burner would be closer to its stoichiometric value and therefore the flame would have a smaller diffusive component. Currently, experimentation is the most used methodology to find the most appropriate shape of the injector. This paper presents an alternative way of finding the injector's geometry by using shape optimisation. Navier Stokes equations written in variational formulation were used to model the flow in the injector/mixer system. The aim was to maximise the primary air entrainment. A shape optimisation method based on Hadamard boundary variation using differentiation with respect to the domain was applied. Results showed improvements of 19.5% in the amount of air dragged into the burner for the optimised injector when compared to the original geometry. The geometry found by the optimisation procedure presents a manufacturability advantage as it requires less tooling to manufacture and allows greater dimensional accuracy. Finally, the method presented is automatic and can be used over any injector-mixer combination, provided that they are axisymmetric. This approach has significant advantages over other experimental or computational methodologies due to its reduced time and cost of development.
2. Keywords: CDF, shape optimisation, Navier-Stokes, gas injector.

3. Introduction
In any combustion system operating with a premixed atmospheric burner, the gas injector (nozzle) is the device responsible for controlling the thermal power and accelerate the fuel gas to generate a low region pressure at the outlet of the nozzle and thus induce the entrainment of the primary air required for the combustion process. Namkhat and Jugjai [1], theoretically established that the primary aeration is a function of fuel flow rate, gas type, nozzle geometry, mixing tube geometry and the burner ports geometry. Therefore, the design of the injector together with the burner is of great importance, as the system must bring a better air-fuel ratio to achieve higher use of the fuel thermal energy and generate lower emissions.
Most conventional domestic burners have high energy losses due to their open flame system which has a relatively low thermal efficiency, less than 30% according to [2, 3]. The traditional design of the nozzles has mainly been based on trial and error tests, where the designer's experience is crucial in selecting the most appropriate form factor. Modern techniques includes the use of experimental setups and computational fluids mechanics. For example, Zhang et al. [4] conducted studies using CFD to improve the gas-air mixture in a premixed burner through the inclusion of an orifice plate in the mixing chamber, resulting in improved uniformity of the velocity at the burner output ports by 234.2 % and fuel–gas mixing by 2.2 %. The results were validated experimentally, showing a reduction of pollutant emissions in the combustion process. They define the objective function as the uniformity of the velocity at the different output ports and use and iterative correction in order to achieve the minimum.
In atmospheric burners, efficient combustion depends largely on the amount of primary air entrained by the jet issuing from a nozzle or orifice [5]. Furthermore, the gas injector shape play an important role in improving air entrainment and the degree of mixing between the fuel jet and the primary air into the mixing tube. For this reason Singh et al. conducted a pilot study with nozzles of circular and non-circular shape to investigate the characteristics of air entrainment from the environment into the mixing tube cross sections [5]. They found that the entrainment ratio increases to a maximum value for small mixing pipe diameters and little separation between the injector and mixer. However, for a larger mixing tube or shifted jet locations, the noncircular jets entrain more of ambient fluid. The results were verified with theoretical approximations made by Pritchard et al. [6] and also with the similarity solution proposed by Becker et al. for circular nozzles [7].
Another important factor to consider in the design of burners, particularly when measuring the primary air entrainment, is the preheating of the air around the burner when it is operating. Namkhat and Jugjai [1] performed

experiments on a self-aspirating burner using both hot and cold tests. They found that the hot test gives about 37% lower primary aeration value than that of the cold test because of the preheating effect caused by combustion.
The optimisation in fluid dynamics has been studied from different points of view and multiple approaches have been developed. The first applications can be seen on minimising the drag on wing profiles [8, 9, 10]. More recently, general optimisation procedures have been applied to the optimisation of problems involving fluids. In [11] Mohammadi and Pironneau present a short survey of optimal shape design (OSD) for fluids. Lohner et al. [12] show developments on shape optimisation for aeronautical applications based on the adjoint method. A gathering of different methods and specific applications is presented on [13] with an engineering emphasis. Shape and topology optimisation for Navier–Stokes problem using variational level set method is presented in [14].
In this paper a shape optimisation method for internal geometry of a gas injector of a premixed atmospheric burner is applied. The objective is to maximise the primary air entrainment. Due to its cylindrical symmetry, the flow is modelled with the Navier Stokes equations in cylindrical coordinates and the optimisation model is based on the Hadamard boundary variation, using differentiation with respect to the domain.

4. Optimisation problem

4.1. Model description

The equivalence ratio, ϕ, is the ratio between the quantities of air and fuel used in a stoichiometric reaction $(A/C)_s$ relative to that used in the actual process $((A/C)_a$, that is

$$\phi = \frac{(A/C)_s}{(A/C)_a} \tag{1}$$

This paper presents a shape optimisation methodology, of the internal shape of the fuel injector, for the minimisation of the equivalence ratio Eq.(1) of a combustion system that uses a premixed atmospheric burner, see Figure 1. The fuel used by the burner is natural gas, for which, according to [15], its stoichiometric air to fuel ratio is equal to $(A/C)_s = 9.52\ \mathrm{m}^3_{\mathrm{air}}\ /\ \mathrm{m}^3_{\mathrm{fuel}}$. Assuming a constant gas flow (k) through the injector, Eq.(1) can be expressed as:

$$\phi = \frac{9.52}{(A/k)_a} \tag{2}$$

Therefore, in order to minimise the equivalence ratio, the amount of air entrainment (A) induced into the burner should be increased. Due to its geometry, a cylindrical coordinate system is used (r, z, θ), with r the radial coordinate, z the coordinate along the axis of the injector/mixer, and θ the angular coordinate along which the properties are assumed constant in this study. The global geometry of the injector-mixer set is described in Figure 1. The assumed working conditions are also shown in the figure. They consist of a developed fuel flow at the entrance of the injector, Γ_{D1}, no slip conditions in the internal walls, Γ_{D2}, radial velocity equal to zero over the axis of symmetry, open boundary conditions at the entrainment zone of the mixer, and open boundary conditions at the exit of the mixer, Γ_N.

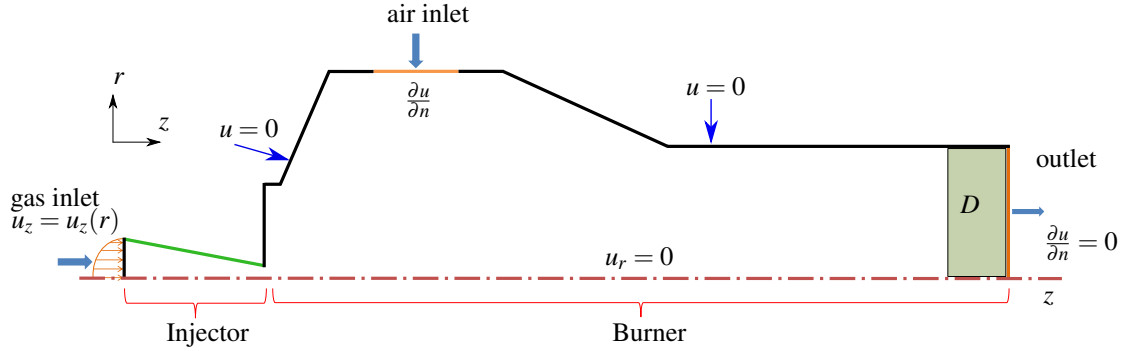

Figure 1: Axisymmetric model of the injector-mixer system used in the optimisation problem

4.2. Mathematical model

Given the fact that minimising the equivalence rate requires the increase in the amount of primary air entering the burner as shown in Eq.(1), and the fuel flow in the injector remains constant, minimising the equivalent rate is identical to increased flow at the output of mixer. Therefore, that can be expressed in terms of a minimisation function by defining a target velocity v_d, whose value is greater that it could be expected at the exit, and minimising the distance of the actual velocity to the target velocity, that is

$$\underset{\Omega \in \mathscr{O}}{\text{minimise}} J(\Omega, u(\Omega)), \quad \text{with} \quad J(\Omega, u(\Omega)) = \int_D |u - u_d|^2 d\Omega \tag{3}$$

where $\mathscr{O}$ is the space of all admissible domains Ω and $D \in \Omega$ is a part of the domain at the exit region where the velocity needs to be maximised. The Cea's method, developed by Jean Cea [16] is proposed to obtain the shape derivative. It is based on the formulation of the Lagrange operator and the solution of the adjoint state equation to find the objective function derivative.
The original problem involves the mixture of two different gasses and the entrainment of air due to the fuel jet. However, in terms of shape optimisation, the problem is equivalent to minimise an air entrainment due to air jet. That is an air-to air problem. This assumption greatly simplifies the physics of the problem and allow us to concentrate on the optimisation algorithm. The complete optimisation problem can be written as

$$\underset{\Omega \in \mathscr{O}}{\text{minimise}} \quad J(\Omega, u(\Omega)) = \int_D |u_i - u_d|^2 d\Omega \tag{4}$$

$$\text{subject to} \begin{cases} R_i(\Omega, u_i, p): & -\nu \Delta u_i + (u_i \cdot \nabla) u_i + \nabla p = 0 \quad \text{in } \Omega \\ C(\Omega, u_i): & \operatorname{div} u_i = 0 \quad \text{in } \Omega \\ & u_i = u_i^D \quad \text{on } \Gamma_{D_1} \\ & \frac{\partial u_i}{\partial n} = 0 \quad \text{on } \Gamma_N \\ & u_r = 0 \quad \text{on } \Gamma_A \\ & u_i = 0 \quad \text{on } \Gamma_{D_2} \end{cases} . \tag{5}$$

The constraints of the problem correspond to the state equation, Eq.(4), plus boundary conditions, Eq.(5). This is an implicit (or nested) formulation of the optimisation problem as the objective function depends on the design variables, which in this case is the domain Ω, and the state variable, the velocity u is also a function of the design variable $u = u(\Omega)$. As the flow can be consider stationary and incompressible, the state equations in Eq.(5) represent the momentum and mass conservation equations. The rest of the constraint correspond to the boundary conditions
As it is a constrained problem, the Lagrangian is defined as

$$\mathscr{L}(\Omega, u_i, p, v_i, q) = J(\Omega, u_i) + \int_\Omega v_i \, R_i(\Omega, u_i, p) \, d\Omega + \int_\Omega q \, C(\Omega, u_i) \, d\Omega \tag{6}$$

where the state equations (R_i) and (C) are incorporated into the Lagrangian function by using the Lagrange multipliers v and q.
Using the first Green identity and taking into account that the momentum and mass conservation equations are written in cylindrical coordinates the weak form of the Eq.(5), can be found as [17]:

$$\begin{cases} a(u_i, v_i) + d(u_i, u_i, v_i) + b(v_i, p) = \displaystyle\int_\Omega f \cdot v_i \, r \, dx \\ \\ b(u_i, q) = 0 \end{cases} \tag{7}$$

where:

$$a(u_i, v_i) = \nu \int_\Omega (\nabla u_i : \nabla v_i) r \, dx + \nu \int_\Omega u_r v_r \frac{1}{r} \, dx \tag{8}$$

$$d(w_i, u_i, v_i) = \int_\Omega ((w_i \cdot \nabla) u_i) \cdot v \, r \, dx \tag{9}$$

$$b(v_i, p) = -\int_\Omega (\operatorname{div} v_i) p \, r \, dx - \int_\Omega v_r \, p \, dx \tag{10}$$

$$b(u_i, q) = -\int_\Omega (\operatorname{div} u_i) q \, r dx - \int_\Omega u_r \, q \, dx \tag{11}$$

The nonlinear convective term, Eq.(9), is linearised using a fixed point like iteration [18, 19]. Therefore, substituting Eq.(8) and Eq.(11) in Eq.(7),the Lagrangian, Eq.(6), is defined as:

$$\begin{aligned} \mathscr{L}(\Omega, u_i, p, v_i, q) = & \int_D |u_i - u_d|^2 \, d\Omega + \nu \int_\Omega (\nabla u_i : \nabla v_i) r \, d\Omega + \nu \int_\Omega u_r v_r \frac{1}{r} \, d\Omega + \int_\Omega (u_o \cdot \nabla u_i) \cdot v_i \, r \, d\Omega \\ & - \int_\Omega (\operatorname{div} v_i) p \, r \, d\Omega - \int_\Omega v_r \, p \, d\Omega - \int_\Omega f \cdot v_i \, r \, d\Omega + \int_\Omega (\operatorname{div} u_i) q \, r d\Omega + \int_\Omega u_r \, q \, d\Omega \end{aligned} \tag{12}$$

The variables v_i and q appear as Lagrange multipliers and act as a test function to obtain the variational formulation

of the state equations R_i and C into $\mathscr{L}$ as shown on Eq.(12). Then, the last two terms of Eq.(6) define the weak form of the state equation. Here u_o is the velocity in the previous iteration.
Finding u_i and p as the solution to the state equation, Eq.(5), one can define the objective function as:

$$J(\Omega) = \mathscr{L}(\Omega, u_i, p, v_i, q) \quad \forall v_i, q \tag{13}$$

According to [20], a variation in the shape of the domain (without topological changes) can be defined with displacement field θ over the initial domain Ω_0. Assuming θ small, a deformed domain Ω is represented as $\Omega = (I+\theta)(\Omega_0)$. Details of the mathematical model are presented in [21] and [22]. Taking into account that definition, the derivative of the function $\mathscr{L}$ with respect to a domain variation in the θ direction is obtained:

$$\begin{aligned}\mathscr{L}'(\Omega, u_i, p, v_i, q)(\theta) = &\frac{\partial \mathscr{L}}{\partial \Omega}(\Omega, u_i, p, v_i, q)(\theta) + \frac{\partial \mathscr{L}}{\partial u_i}(\Omega, u_i, p, v_i, q)(\dot{u}_i(\theta)) \\ &+ \frac{\partial \mathscr{L}}{\partial p}(\Omega, u_i, p, v_i, q)(\dot{p}(\theta)) + \frac{\partial \mathscr{L}}{\partial v_i}(\Omega, u_i, p, v_i, q)(\dot{v}_i(\theta)) \\ &+ \frac{\partial \mathscr{L}}{\partial q}(\Omega, u_i, p, v_i, q)(\dot{q}(\theta))\end{aligned} \tag{14}$$

This result is obtained taking advantage of the non dependancy of the variables (u_i, p, v_i, q) on the domain. The partial derivatives with respect to these variables, that are different from the domain, are calculated as follows:

$$\begin{aligned}&\frac{\partial \mathscr{L}}{\partial u_i}(\Omega, u_i, p, v_i, q)(\dot{u}_i(\theta)) \rightarrow \\ &\partial_\lambda \mathscr{L}(\Omega, u_i + \lambda \widehat{u}_i, p, v_i, q)|_{\lambda=0} = J'(u_i, \widehat{u}_i) + \nu \int_\Omega (\nabla \widehat{u}_i : \nabla v_i) r \, d\Omega + \nu \int_\Omega \widehat{u}_r v_r \frac{1}{r} \, d\Omega \\ &\qquad + \int_\Omega (u_o \cdot \nabla \widehat{u}_i) \cdot v_i \, r \, d\Omega + \int_\Omega (\operatorname{div} \widehat{u}_i) q \, r d\Omega + \int_\Omega \widehat{u}_r \, q \, d\Omega\end{aligned} \tag{15}$$

$$\frac{\partial \mathscr{L}}{\partial p}(\Omega, u_i, p, v_i, q)(\dot{p}(\theta)) \rightarrow \partial_\lambda \mathscr{L}(\Omega, u_i, p + \lambda \widehat{p}, v_i, q)|_{\lambda=0} = -\int_\Omega (\operatorname{div} v_i) \widehat{p} \, r \, d\Omega - \int_\Omega v_r \, \widehat{p} \, d\Omega \tag{16}$$

$$\begin{aligned}&\frac{\partial \mathscr{L}}{\partial v_i}(\Omega, u_i, p, v_i, q)(\dot{v}_i(\theta)) \rightarrow \\ &\partial_\lambda \mathscr{L}(\Omega, u_i, p, v_i + \lambda \widehat{v}_i, q)|_{\lambda=0} = \nu \int_\Omega (\nabla u_i : \nabla \widehat{v}_i) r \, d\Omega + \nu \int_\Omega u_r \widehat{v}_r \frac{1}{r} \, d\Omega \\ &\qquad + \int_\Omega (u_o \cdot \nabla u_i) \cdot \widehat{v}_i \, r \, d\Omega - \int_\Omega (\operatorname{div} \widehat{v}_i) p \, r \, d\Omega - \int_\Omega \widehat{v}_r \, p \, d\Omega\end{aligned} \tag{17}$$

$$\frac{\partial \mathscr{L}}{\partial q}(\Omega, u_i, p, v_i, q)(\dot{q}(\theta)) \rightarrow \partial_\lambda \mathscr{L}(\Omega, u_i, p, v_i, q + \lambda \widehat{q})|_{\lambda=0} = \int_\Omega (\operatorname{div} u_i) \widehat{q} \, r d\Omega + \int_\Omega u_r \, \widehat{q} \, d\Omega \tag{18}$$

The derivative of the objective function, $J'(u)$, is calculated as:

$$J'(u_i, \widehat{u}_i) = \int_D 2(u_i - u_d) \, \widehat{u}_i \, d\Omega \tag{19}$$

Equations Eq.(17) and Eq.(18) correspond to the weak form of the momentum and continuity equations and they solve for u_i and p), for any arbitrary $\widehat{v}_i$ and $\widehat{q}$ test functions. on the other hand, equations Eq.(15) and Eq.(16) correspond to the adjoint system. Eq.(15) has the same form of the state equation with a source term defined by the derivative of the objective function J'. In this case, one solves the state equation for the variables (u_i, p) and then they are used to compute the source term J' and them the adjoint system is solve for the variables (v_i, q). Finally, after making all these terms null, the shape derivative, Eq.(14), reads:

$$\mathscr{L}'(\Omega, u_i, p, v_i, q)(\theta) = \frac{\partial \mathscr{L}}{\partial \Omega}(\Omega, u_i, p, v_i, q)(\theta) \tag{20}$$

The partial derivative $\partial \mathscr{L} / \partial \Omega$ is computed using the Structure Theorem, see [16], [23, theorem 3.6 p. 479] and [22, theorem 2.2.2] for a detail explanation.

$$\begin{aligned}\frac{\partial \mathscr{L}}{\partial \Omega}(\Omega, u_i, p, v_i, q)(\theta) = \int_{\partial \Omega_0} \theta \cdot \widehat{n}_i (&|u_i - u_d|^2 + \nu \, (\nabla u_i : \nabla v_i) r + \nu \, u_r v_r \frac{1}{r} + (u_i \cdot \nabla u_i) \cdot v_i \, r \\ &- (\operatorname{div} v_i) p \, r - v_r \, p - f \cdot v_i \, r + (\operatorname{div} u_i) q \, r + u_r \, q) \, ds,\end{aligned} \tag{21}$$

where $\hat{n}_i$ is the unitary vector that defines the normal direction of $\partial\Omega_0$. The terms (v_i, q) are the solution to the adjoint system defined by Eq.(15) and Eq.(16). The shape derivative can be defined as the sensitivity of the objective function $J(\Omega)$ with respect to a variation of the domain shape defined by the boundary displacement field of magnitude θ on the normal direction $\hat{n}_i$.
This model was implemented using FreeFem++ [24] using the initial geometry shown in 1. The visualisation of the results is accomplished exporting the results into VTK format and visualising into ParaView.

5. Results

The minimum diameter of the injector defines the thermic power of the burner. Therefore, in order to preserve the thermic power of the system an additional restriction was set to ensure that the smallest dimension in the radial direction was not less than a given value.
The optimisation problem defined by Eq.(4) and Eq.(5) was implemented with a initial geometry as shown in figure 1. Although the sensitivity was calculated for any point in Ω only the shape of the injector was allowed to evolve. The variation on the boundary was accomplished according to the shape derivative defined in Eq.(21). Each iteration involves the computation of the shape sensitivity, a correction in the injector shape, remeshing of the injector domain and computation of the new objective function
Figure 2 presents the initial and optimised injector geometries, the evolution of the optimisation function and the variation of air entrainment. It can be observed that, as expected, the objective function decreases and the amount of primary air drawn into the burner increases. Only eight iterations were required until the minimum diameter of the injector reached its minimum limit, so it can guaranty the required thermic power of the burner.

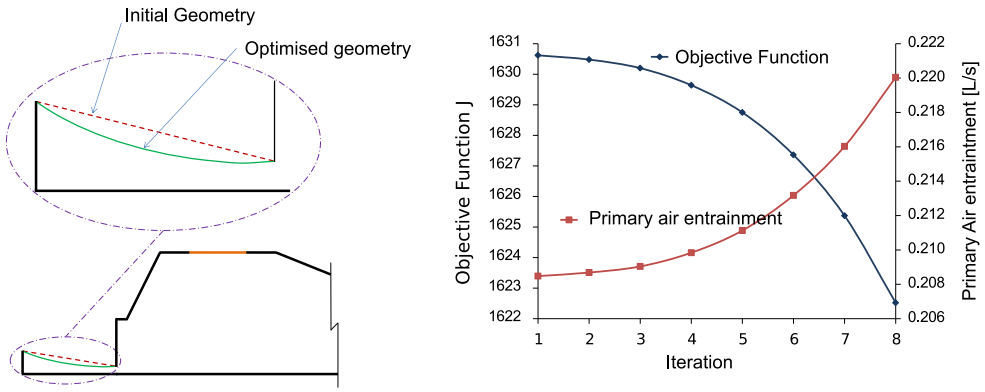

Figure 2: Left: Initial geometry and its final shape after running the optimisation algorithm. Right: behaviour of the objective function and the air flow entrainment at each iteration

In Figure 3 the geometries of both, the original injector and the found by the optimisation procedure are compared. The original geometry refers to the current design of the injector that has led to the study in this paper. A comparison of the flow field in the original and the optimised injector is shown. Figure 3a presents the velocity field on the original injector, a balance of the flows and a scale showing the magnitude of the velocity. Likewise, Figure 3b presents the same information for the optimised injector. The fields were calculated solving Eq.(5) for each of the geometries. It can be appreciated that the velocity at the output is larger for the optimised model. Also the primary air entrainment is increased from $Q_d = 0.184182$ L/s for the original one to $Q_d = 0.220038$ L/s to the optimised one. That is equivalent to an increment of the 19.5% and maintaining the same level of flow at the injector input. From the manufacturability point of view, it can be observed that the construction of the optimised shape is easy compared with the current design as it requires less tooling and manufacturing processes.

5. Conclusions

The shape optimisation method using shape derivatives, has been successfully applied to optimise the equivalence rate on a gas injector of an atmospheric burner. The objective function was written in terms of minimising the distance of the velocity to a target velocity at the outlet. A shape optimisation method based on Hadamard boundary variation using differentiation with respect to the domain was applied. The results showed improvements of 19.5% in the primary air entrainment when compared to the previous geometry. This implies a combustion system with higher thermal efficiency and lower emissions. Additionally, the geometry found by the optimisation procedure

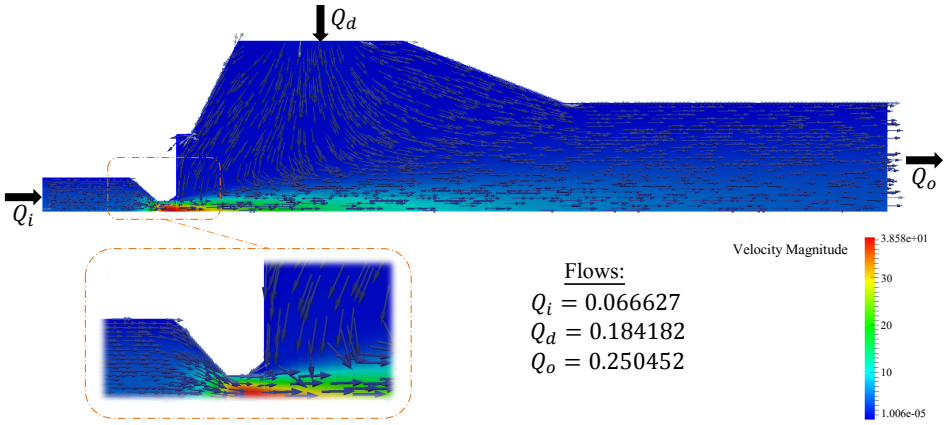

(a) Velocity field and summary of flows for the original injector

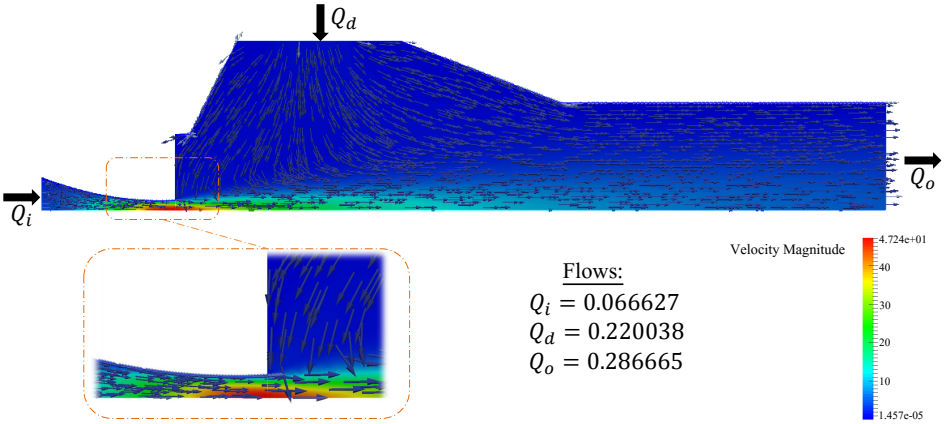

(b) Velocity field and summary of flows for the optimised injector

Figure 3: Comparison of the flow fields in the original and optimised injector.

presents a manufacturability advantage as it requires less tooling to manufacture and allows greater dimensional accuracy. Finally, the method presented is automatic and can be used over any injector-mixer combination, provided that they are axisymmetric. This approach has significant advantages over other experimental or computational methodologies due to its reduced time and cost of development.

6. Acknowledgements

This work was supported by EAFIT University, Industrias HACEB and COLCIENCIAS (Colombia) under research grant No 1216-562-37637.

7. References

[1] A. Namkhat and S. Jugjai. Primary air entrainment characteristics for a self-aspirating burner: Model and experiments. *Energy*, 35(4):1701–1708, April 2010.

[2] S Jugjai, S Tia, and N Rungsimuntuchart. Experimental Study on Efficiency Heat -recirculating Gas Burners Based on the Porous Medium Technology. *Asian J. Energy Environ*, 2:169–198, 2001.

[3] Sumrerng Jugjai and Natthawut Rungsimuntuchart. High efficiency heat-recirculating domestic gas burners. *Experimental Thermal and Fluid Science*, 26(5):581–592, July 2002.

[4] Tian Hu Zhang, Feng Guo Liu, and Xue Yi You. Optimization of gas mixing system of premixed burner based on CFD analysis. *Energy Conversion and Management*, 85:131–139, 2014.

[5] Ghanshyam Singh, T. Sundararajan, and K. a. Bhaskaran. Mixing and Entrainment Characteristics of Circular and Noncircular Confined Jets. *Journal of Fluids Engineering*, 125(September 2003):835, 2003.

[6] Robert Prichard, J.J. Guy, and N.E. Connor. *Handbook of Industrial Gas Utilization*. Van Nostrand Reinhold Co., New Providence, NJ., 1997.

[7] H. A. Becker, H. C. Hottel, and G. C. Williams. Mixing And Flow in Ducted Turbulent Jets. In *9th Int. Symp. Combustion, The Combustion Institute*, pages 7–20, Pittsburgh, 1963. Academic Press.

[8] Juan J. Alonso, Juan J. Alonso, Ilan M. Kroo, Ilan M. Kroo, Antony Jameson, and Antony Jameson. Advanced algorithms for design and optimization of quiet supersonic platforms. *of*, 14, 2002.

[9] F. Bauer, P. Garabedian, D. Korn, and A. Jameson. *Supercritical Wing Sections*. Springer, Berlin, 1977.

[10] O. Pironneau. On optimum design in fluid mechanics. *Journal of Fluid Mechanics*, 64:97–110, 6 1974.

[11] B. Mohammadi and O. Pironneau. Applied optimal shape design. *Journal of Computational and Applied Mathematics*, 149(1):193 – 205, 2002. Scientific and Engineering Computations for the 21st Century - Methodologies and Applications Proceedings of the 15th Toyota Conference.

[12] R Löhner, O Soto, and C Yang. An adjoint-based design methodology for CFD optimization problems. *School of computational science*, 2003.

[13] Dominique Thvenin and Gbor Janiga. *Optimization and Computational Fluid Dynamics*. Springer Publishing Company, Incorporated, 1st edition, 2008.

[14] Xian-Bao Duan, Yi-Chen Ma, and Rui Zhang. Shape-topology optimization for navier–stokes problem using variational level set method. *Journal of Computational and Applied Mathematics*, 222(2):487 – 499, 2008.

[15] Andrés Amell Arrieta. Estimación de las propiedades de combustión de combustibles gaseosos. Technical report, Universidad de Antioquia, Medellín, 2002.

[16] Jean Céa. Conception optimale ou identification de formes: calcul rapide de la dérivée directionnelle de la fonction coût. *Modélisation mathématique et analyse numérique*, 20:371–402, 1986.

[17] Simone Deparis. *Numerical Analysis of Axisymmetric Flows and Methods for Fluid-Structure Interaction Arising in Blood Flow Simulation*. PhD thesis, École polytechnique fédérale de Lausanne, 2004.

[18] Wolfgang A. Wall. *Fluid-Struktur-Interaktion mit stabilisierten Finiten Elementen*. PhD thesis, University Stuttgart, 1999.

[19] Volker Gravemeier. *The Variational Multiscale Method for Laminar and Turbulent Incompressible Flow Volker Gravemeier*. PhD thesis, Stuttgart University, 2003.

[20] Jacques Hadamard. *Mémoire sur le problème d'analyse relatif à l'équilibre des plaques élastiques encastrées*. Mémoires présentés par divers savants l'Académie des sciences de l'Institut de France: Éxtrait. Imprimerie nationale, Paris, 1908.

[21] Grégoire Allaire. *Conception optimale de structures: Majeure Sciences de l'ingénieur, simulation et modélisation*. École polytechnique, Département de Mathématiques appliquées, 2006.

[22] Charles Dapogny. *Shape optimization, level set methods on unstructured meshes and mesh evolution*. PhD thesis, École Doctorale Paris Centre, 2013.

[23] M. C. Delfour and J.-P. Zolésio. *Shapes and Geometries: Metrics, Analysis, Differential Calculus and Optimization*. SIAM, 2nd edition, 2011.

[24] F Hecht. New development in FreeFem++. *J. Numer. Math.*, 20(3-4):251–265, 2012.